AFRL-VS-TR-2000-1513

Improvements to the PRISM and PIM Ionospheric Models

Robert E. Daniell, Jr.

Computational Physics, Inc.
207 Fulton Street
Norwood, MA 02062

26 August 1999

Final Report
(11 Aug 97-10 Aug 99)

AIR FORCE RESEARCH LABORATORY
Space Vehicles Directorate
29 Randolph Rd
AIR FORCE MATERIEL COMMAND
Hanscom AFB, MA 01731-3010

This technical report has been reviewed and is approved for publication.

PETER J. SULTAN
Contract Manager, VSBXP

GREGORY P. GINET
Branch Chief, VSBXT

ROBERT A. MORRIS
Division Chief, VSB

This report has been reviewed by the ESC Public Affairs Office (PA) and is releasable to the National Technical Information Service (NTIS).

Qualified requestors may obtain additional copies from the Defense Technical Information Center (DTIC). All others should apply to the National Technical Information Service (NTIS).

If you change your address, wish to be removed from this mailing list, or your organization no longer employs the addressee, please notify AFRL/VSRTM, 29 Randolph Road, Hanscom AFB, MA 01731-1010. This will assist us in maintaining a current mailing list.

Do not return copies of this report unless contractual obligations or notices on a specific document require that it be returned.

REPORT DOCUMENTATION PAGE

Form Approved
OMB No. 0704-0188

1. AGENCY USE ONLY (*Leave blank*)	2. REPORT DATE	3. REPORT TYPE AND DATES COVERED
	August 1999	Final (11 Aug 97 – 10 Aug 99)

4. TITLE AND SUBTITLE
Improvements to the PRISM and PIM Ionospheric Models

5. FUNDING NUMBERS
PE 63790F
PR 4026 TA GL WU MD

Contract F19628-95-C-0079

6. AUTHOR(S)
Robert E. Daniell, Jr.

7. PERFORMING ORGANIZATION NAME(S) AND ADDRESS(ES)
Computational Physics, Inc.
207 Fulton Street
Norwood, MA 02062-2707

8. PERFORMING ORGANIZATION REPORT NUMBER

9. SPONSORING / MONITORING AGENCY NAME(S) AND ADDRESS(ES)
Air Force Research Laboratory
29 Randolph Road
Hanscom AFB, MA 01731-3010
Contract Manager: Peter Sultan/VSBP

10. SPONSORING / MONITORING AGENCY REPORT NUMBER
AFRL-VS-TR-2000-1513

11. SUPPLEMENTARY NOTES

12A. DISTRIBUTION / AVAILABILITY STATEMENT
APPROVED FOR PUBLIC RELEASE;
DISTRIBUTION UNLIMITED

12b. DISTRIBUTION CODE

13. ABSTRACT (*Maximum 200 words*)

This report describes updates that have been made to the Parameterized Real-time Ionospheric Specification Model (PRISM) that is operational at the 55th Space Weather Squadron (55 SWXS). It also describes a modified TEC data assimilation algorithm that has been implemented in a special regional version of PRISM, and which is available for implementation in the operational version. Finally, it describes several activities related to the validation of PRISM using data from a variety of sources.

14. SUBJECT TERMS
Ionosphere, Space environment, Data assimilation, Space weather, Ionospheric specification

15. NUMBER OF PAGES
31

16. PRICE CODE

17. SECURITY CLASSIFICATION OF REPORT	18. SECURITY CLASSIFICATION OF THIS PAGE	19. SECURITY CLASSIFICATION OF ABSTRACT	20. LIMITATION OF ABSTRACT
Unclassified	Unclassified	Unclassified	SAR

Table of Contents

Executive Summary

Due to a lower level of funding than originally anticipated, the emphasis of this contract has been on supporting the existing version of the Parameterized Real-time Ionospheric Specification Model (PRISM) by providing incremental improvements, updates, and bug fixes rather than developing major new capabilities. CPI has also provided technical support to AFRL personnel engaged in a major effort to validate PRISM as it exists at the 55th Space Weather Squadron.

The primary incremental improvement was the implementation of a modified TEC data assimilation algorithm that makes more intelligent use of TEC data when it is in the vicinity of ionosonde data. The algorithm has been implemented in a special version of PRISM and tested with ionosonde data from Chilton, UK and IMS TEC data from nearby Croughton, UK.

PRISM 1.7c was delivered to the 55th Space Weather Squadron after revalidation using the same data set that was used to validate PRISM 1.2.

1. INTRODUCTION

The original objective of this contract was to develop and implement several substantial improvements to the Parameterized Real-time Ionospheric Specification Model (PRISM) leading to a new version. Among the planned improvements were (1) improving PRISM's base climatology, i.e., the Parameterized Ionospheric Model (PIM), (2) extending PRISM (and PIM) to include the plasmasphere, and (3) improving PRISM's data assimilation algorithm. The first two objectives involved parameterizing a single, global, physics-based, multi-ion ionospheric model (AFRL's Global Theoretical Ionospheric Model, GTIM) instead of the separate regional ionospheric models used in the original PRISM development effort. A secondary objective of this contract was the continued support of the operational version of PRISM at the 55th Space Weather Squadron at Schriever (formerly Falcon) AFB, including the development of PRISM applications such as three dimensional ray tracing software or visualization software for use with PRISM output, and the development of data fusion algorithms to improve the accuracy and scope of data derived from the various space environment sensors on DMSP satellites.

Due to the limited availability of funding for this contract, these objectives had to be scaled back. The data fusion task was specifically eliminated, and the overall effort was directed toward more modest goals. Nevertheless, significant progress toward developing PRISM 2 has been made. A multi-ion version of GTIM was developed, although it only applies to low and midlatitudes – the high latitude version of GTIM developed by Dwight Decker at AFRL remains a separate code. This accomplishment has been described by *Daniell et al.* [1998] and *Daniell and Brown* [1998]. There is, however, a difficulty with using GTIM (or similar, ambipolar-based codes) to model the plasmasphere. These issues are discussed in Appendix B.

The modification of VOACAP to read and use PRISM output was completed under this contract and described by *Daniell et al.* [1998]. Since that time, CPI has assisted 55 SWXS in the installation and testing of the modified VOACAP on their computers.

During the course of this contract a number of modifications have been made to PRISM to enhance its performance or to correct problems reported by PIM and PRISM users, including AFRL personnel. These changes are documented in Appendix A of this report.

At the instigation of – and under the supervision of – AFRL personnel, CPI produced a version of PRISM intended for regional applications with a modified TEC data assimilation algorithm. This algorithm and issues related to its implementation in the full global version of PRISM are described in Section 2 below.

Finally, CPI has participated in various PRISM validation efforts: (a) validation of PRISM 1.7c (the current version at 55 SWXS), (b) validation of the regional version, and (c) the more thorough PRISM validation effort being led by Dr. Dwight Decker of AFRL (formerly of Boston College). CPI's contributions to these efforts are described in Section 3.

2. PRISM ASSIMILATION OF TEC DATA

A long standing problem related to data assimilation in PRISM is the use of Total Electron Content (TEC) data. PRISM's data assimilation algorithm has always been oriented toward the use of "point" measurements from ground-based ionosonde data or space-based *in situ* data from satellites. The use of an integrated quantity such as TEC is problematic in this scheme. The problem arises because PRISM assimilates data by directly adjusting the vertical electron density profiles (EDPs) themselves. Incorporating slant TEC measurements in this scheme is difficult because it is not clear how to assign adjustments to each of the vertical EDPs that are sampled by the TEC measurement.

The approach taken in the present version of PRISM was to require that all slant TEC measurements be converted to "vertical equivalent TEC" measurements. PRISM does not prescribe the method to be used for this conversion, but the conventional method is the thin shell approximation. The ionosphere is assumed to be concentrated in a thin layer at a constant altitude. (Some people use 350 km, the approximate altitude of the peak density in the daytime in midlatitudes, while others use 420 km, the approximate height of the centroid of the electron density in midlatitudes.) The intersection of the line-of-sight and the thin shell (the Ionospheric Pierce Point or IPP) defines the location to which the vertical equivalent TEC is assigned. The value of the vertical TEC is calculated from

$$\text{Vertical Equivalent TEC} = \text{Slant TEC} \times \cos\chi$$

where χ is the zenith angle of the line-of-sight at the IPP. All PRISM requires is the latitude and longitude of the IPP and the calculated vertical equivalent TEC.

Data assimilation in PRISM takes place in three Steps. In Step 1 all information on the height of the *E*- and *F*-layers is assembled and used to construct correction fields for h_mE and h_mF_2 that describe, as a function of latitude and longitude, the amounts by which PRISM's climatological EDP's must be shifted to match the data. Step 1 is complete once the calculated correction field has been to the original EDPs. In Step 2 all the information on the magnitude of the peak density of the *E*- and *F*-layers is assembled and used to construct correction fields for f_oE and f_oF_2 that describe the amounts by which the PRISM EDPs must be corrected to match the data. For ionosonde data this process is relatively straightforward. The correction field for the critical frequencies is constructed from the difference of the measured and model values:

$$\Delta f_oF_2 = f_oF_2^{measured} - f_oF_2^{modeled}$$
$$\Delta f_oE = f_oE^{measured} - f_oE^{modeled}$$

In order to make use of the TEC data within PRISM's present data assimilation algorithm, it must be converted from an integrated measurement to a point measurement. For TEC, PRISM does this by scaling the entire EDP by the ratio of the observed TEC to the modeled TEC. Then it generates a pseudo-ionosonde data record by reading the peak densities off the scaled EDP and converting them to critical frequencies.

$$R_{TEC} = \frac{\text{observed TEC}}{\text{modeled TEC}}$$

$$N_m F_2^{corrected} = R_{TEC} \times N_m F_2^{modeled}$$
$$N_m E^{corrected} = R_{TEC} \times N_m E^{modeled}$$

$$f_o F_2^{corrected} = \sqrt{R_{TEC}} \times f_o F_2^{modeled}$$
$$f_o E^{corrected} = \sqrt{R_{TEC}} \times f_o E^{modeled}$$

At this point PRISM constructs the complete critical frequency correction fields for the *E*- and *F*-layers. The final step, Step 3, involves the construction of correction fields for the topside profile parameters, the electron density and the plasma scale height at 840 km.

There are several problems with this approach. First, because the topside EDP corrections are constructed so as to preserve the peak densities, they do not preserve TEC. Thus, if *in situ* plasma data is available, PRISM will no longer reproduce the TEC observations. The second problem occurs when there are TEC measurements in close proximity to ionosonde measurements. The values of $f_o F_2$ and $f_o E$ derived from the TEC measurements will generally not agree with the values directly measured by the ionosonde. The result is the possibility of spurious gradients in the region between the ionosonde and TEC measurements.

The documentation for PRISM 1.5 [*Daniell and Brown*, 1995] prescribes a solution for the second problem, which also mitigates the first problem to some degree. Specifically, when the TEC measurements fall within some prescribed distance from an ionosonde measurement, they are to be used to modify the topside EDP rather than the peak densities. Unfortunately, due to various difficulties – technical, financial, and managerial – this solution was never implemented. When AFRL decided to use PRISM for a specific regional application in which a DISS sensor and an IMS sensor were to be collocated, it became imperative that the ionosonde and TEC data be assimilated in a consistent manner.

In essence, the algorithm works by deriving a pseudo-SSIES data record for each TEC profile. The SSIES algorithm, based on knowledge of two data, N_{top} (measured at altitude z_{top}) and the scale height H_{top} (also measured at altitude z_{top}), dictates

$$N_c(z) = N_m(\zeta) \tag{1}$$

where $N_c(z)$ is the *corrected* (Step 3) model electron density at altitude z and $N_m(\zeta)$ is the model electron density at altitude ζ (*after* Step 2 corrections). The altitude ζ is determined from

$$\zeta(z)=\begin{cases} z, & z \le h_m F_2 \\ h_m F_2 + \left[2\dfrac{z_1 - h_m F_2}{z_{top} - h_m F_2} - \dfrac{H_m(z_1)}{H_{top}} \right](z - h_m F_2) + \left[\dfrac{H_m(z_1)}{H_{top}} - \dfrac{z_1 - h_m F_2}{z_{top} - h_m F_2} \right] \dfrac{(z - h_m F_2)^2}{z_{top} - h_m F_2}, & z > h_m F_2 \end{cases} \quad (2)$$

with the altitude z_1 specified by the condition

$$N_m(z_1) = N_{top} \quad (3)$$

and the scale height at z_1, $H_m(z_1)$, defined as

$$\frac{1}{H_m(z_1)} = -\left(\frac{1}{N_m} \frac{\partial N_m}{\partial z} \right)_{z=z_1} \quad (4)$$

In the case of a TEC measurement, rather than an SSIES measurement, we have no datum with which to specify the scale height, so we are free to assign it so that the quadratic coefficient vanishes:

$$\frac{H_m(z_1)}{H_{top}} = \frac{z_1 - h_m F_2}{z_{top} - h_m F_2} \quad (5)$$

or

$$H_{top} = \frac{z_{top} - h_m F_2}{z_1 - h_m F_2} H_m(z_1) \quad (6)$$

Consequently, the altitude scaling becomes

$$\zeta(z)=\begin{cases} z, & z \le h_m F_2 \\ h_m F_2 + \dfrac{z_1 - h_m F_2}{z_{top} - h_m F_2}(z - h_m F_2), & z > h_m F_2 \end{cases} \quad (7)$$

To derive a pseudo-SSIES correction from TEC, we determine z_1 by replacing the condition $N_m(z_1) = N_{top}$ with the condition

$$TEC_{IMS} = \int_0^{z_\infty} N_c(z')dz' = \int_0^{z_\infty} N_m(\zeta)dz' \quad (8)$$

or

$$TEC_{IMS} = \int_0^{h_mF_2} N_m(z')dz' + \int_{h_mF_2}^{z_\infty} N_m(\zeta)dz' \tag{9}$$

If we change the integration variable from z' to ζ, then we may use

$$z' = h_mF_2 + \frac{z_{top} - h_mF_2}{z_1 - h_mF_2}(\zeta - h_mF_2) \tag{10}$$

so that

$$dz' = \frac{z_{top} - h_mF_2}{z_1 - h_mF_2}d\zeta \tag{11}$$

and the limits of integration change from $[h_mF_2, z_\infty]$ to $[h_mF_2, \zeta_\infty]$ where

$$\zeta_\infty = \zeta(z_\infty) = h_mF_2 + \frac{z_1 - h_mF_2}{z_{top} - h_mF_2}(z_\infty - h_mF_2) \tag{12}$$

Thus, we have

$$TEC_{IMS} = \int_0^{h_mF_2} N_m(z')dz' + \frac{z_{top} - h_mF_2}{z_1 - h_mF_2}\int_{h_mF_2}^{\zeta_\infty} N_m(\zeta)d\zeta \tag{13}$$

Since the nominal TEC value given by the model is

$$TEC_m = \int_0^{h_mF_2} N_m(z')dz' + \int_{h_mF_2}^{z_\infty} N_m(z')dz' \tag{14}$$

the difference is:

$$\Delta TEC = TEC_{IMS} - TEC_m = \frac{z_{top} - h_mF_2}{z_1 - h_mF_2}\int_{h_mF_2}^{\zeta_\infty} N_m(\zeta)d\zeta - \int_{h_mF_2}^{z_\infty} N_m(z')dz' \tag{15}$$

If we let $z_\infty \to \infty$, then $\zeta_\infty \to \infty$, and the difference becomes

$$\Delta TEC = TEC_{IMS} - TEC_m = \left[\frac{z_{top} - h_mF_2}{z_1 - h_mF_2} - 1\right]\int_{h_mF_2}^{\infty} N_m(z')dz' \tag{16}$$

or

$$\Delta TEC = TEC_{IMS} - TEC_m = \left[\frac{z_{top} - z_1}{z_1 - h_m F_2}\right] \int_{h_m F_2}^{\infty} N_m(z')dz' \tag{17}$$

Let $TEC_{top} = \int_{h_m F_2}^{\infty} N_m(z)dz$. Then z_1 is determined by

$$\frac{z_{top} - z_1}{z_1 - h_m F_2} = \frac{\Delta TEC}{TEC_{top}} \tag{18}$$

or

$$z_1 = \frac{TEC_{top} \cdot z_{top} + \Delta TEC \cdot h_m F_2}{TEC_{top} + \Delta TEC} \tag{19}$$

from which we may determine the topside scale height:

$$\begin{aligned} H_{top} &= \frac{z_{top} - h_m F_2}{z_1 - h_m F_2} H_m(z_1) \\ &= \left[\frac{z_{top} - z_1 + (z_1 - h_m F_2)}{z_1 - h_m F_2}\right] H_m(z_1) \\ &= \left[1 + \frac{z_{top} - z_1}{z_1 - h_m F_2}\right] H_m(z_1) \end{aligned}$$

or

$$H_{top} = \left[1 + \frac{\Delta TEC}{TEC_{top}}\right] H_m(z_1) \tag{20}$$

In other words, given the nominal model value of TEC (TEC_m) and the measured value of TEC (TEC_{IMS}), we may determine values for z_1 and H_{top} that, when fed to the SSIES algorithm, will result in a corrected topside profile that yields the measured value of TEC.

This algorithm has been implemented and is available for inclusion the official version of PRISM when it is approved by AFRL and AFSPC.

In the meantime, the new TEC data assimilation algorithm is available for implementation in the operational version of PRISM.

3. PRISM VALIDATION

Under this contract, CPI engaged in three different activities related to PRISM validation. These activities were (a) the revalidation of PRISM 1.7b and PRISM 1.7c using a standard data set first assembled for the validation of PRISM 1.2, (b) verification and validation of the modified TEC data assimilation algorithm described in the previous section, and (c) participating in a comprehensive validation effort being led by Dr. D. T. Decker of AFRL. Each of these activities is described in this section.

3.1 Revalidation of PRISM 1.7b and 1.7c

At the request of Air Force Space Command (AFSPC) and AFRL, CPI conducted a revalidation of PRISM 1.7b and PRISM 1.7c using the same data set used to validate PRISM 1.2 [*Daniell et al.*, 1994]. While this data set was rather limited, covering only a few days in October 1989, its use demonstrated that the changes made in moving from Version 1.2 to Version 1.7 had not degraded PRISM's overall performance. This was expected, since most of the changes were made to correct specific problems that had been identified by various users. However, by no means does the data set constitute a comprehensive validation data set for PRISM.

The PRISM 1.7b validation results were summarized in a CPI report dated 28 August 1997, and the PRISM 1.7c validation results were summarized in a CPI report dated 3 January 1998. These reports are reproduced in Appendix C.

3.2 Verification and Validation of Modified TEC Algorithm

The second validation activity involved the validation of the TEC assimilation algorithm described in the previous section. The algorithm was tested using actual data from the Digisonde operated by the Rutherford Appleton Laboratory (RAL) at Chilton, UK (51.5ºN,0.6ºW), and the IMS instrument operated by AFRL at Croughton, UK (52.0ºN,1.2ºW). For the purpose of verification of the algorithm, data from a single 24 hour period were used: 2 April (day 92) of 1998. The Chilton Digisonde data were obtained from the RAL web site. The Chilton data were supplied by G. Bishop of AFRL and A. Mazzella of NWRA. The satellite with the highest elevation in each 15 minute time interval was used to obtain vertical equivalent TEC for input to PRISM. The other satellites were processed separately to provide "truth".

The performance of the algorithm was assessed by making four different PRISM runs: (1) No input data, (2) Digisonde ("DISS") data only, (3) IMS data only, and (4) both Digisonde and IMS data. In each case, PRISM slant TEC along the lines-of-sight to the "truth" satellites was compared to the observed slant TEC. Both differences and ratios were calculated. The results are displayed on the next page. While it is dangerous to draw conclusions from a limited data set, the new algorithm for assimilating TEC data in the vicinity of DISS data does seem to be of benefit. Even though the mean ratio is slightly worse than for IMS alone, the scatter in the data appears to be smaller.

No Data

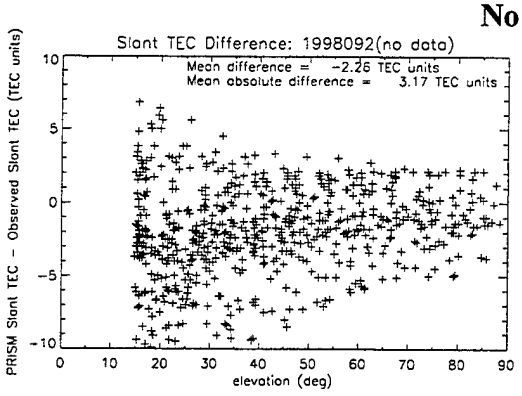

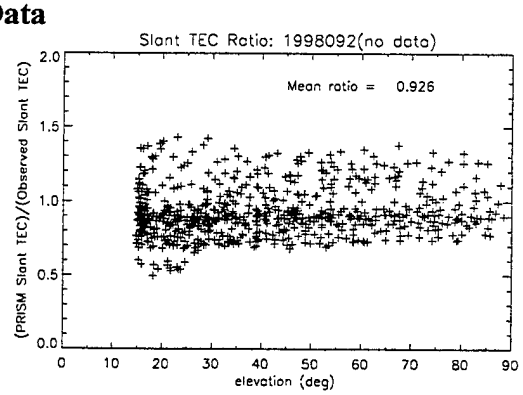

DISS only

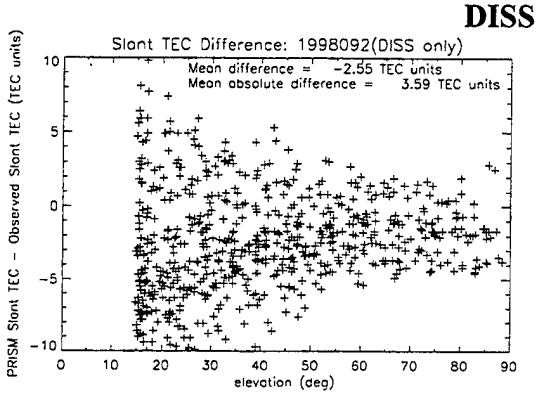

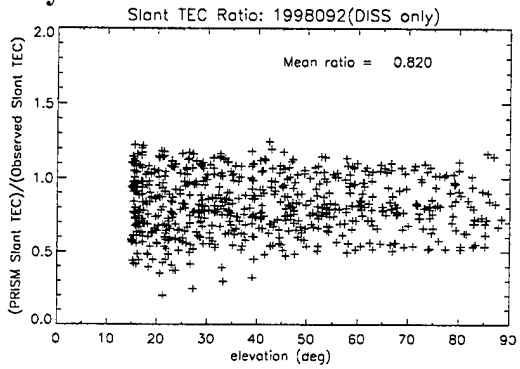

IMS only

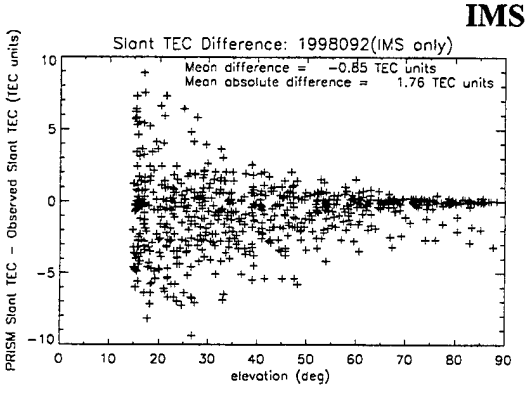

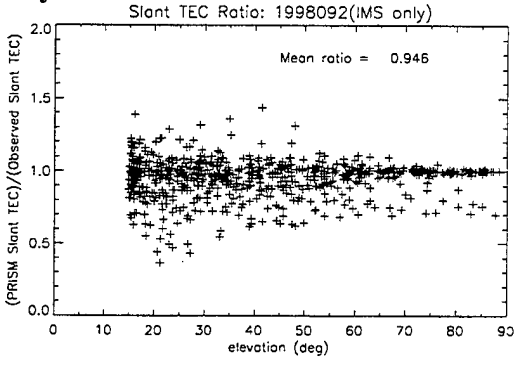

DISS & IMS

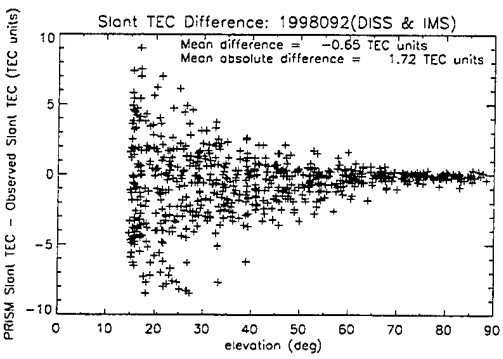

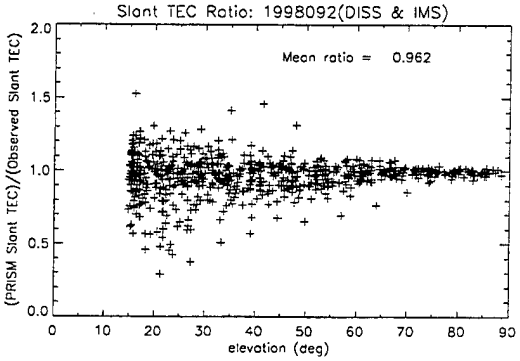

The results also raise some questions that should be investigated in the future. Besides performing a more detailed statistical analysis (e.g., calculating variance as a function of elevation angle), the source of the outliers at high elevation angles in the "IMS only" case needs to be understood to insure that the algorithm has been correctly implemented.

3.3 Participation in AFRL's Comprehensive Validation Effort

CPI has assisted in the comprehensive PRISM validation effort being led by Dr. D. T. Decker of AFRL. Besides providing technical support related to the installation and operation of PRISM 1.7c on AFRL computers and responding to questions and problems identified by AFRL personnel, CPI has undertaken validation studies using GPS slant TEC data. An example was the use of data from a GPS receiver at Bermuda. These data were supplied by P. Doherty of Boston College. As in the regional model validation described above, the GPS satellite at the highest elevation was used as input to PRISM while the other satellites in view provided "truth" data for comparison with PRISM predictions.

For the initial validation runs, data from the set used by *Coxwell* [1997] was selected. This data set was chosen because it permits a direct comparison with his results, and because the data had already been carefully quality controlled by Ms. Doherty. Unfortunately, an elevation mask of 40° was applied to that data, so it does not provide as much areal coverage as would be ideal. Nevertheless, it remains a useful data set. The first validation runs used data from Bermuda taken on 9 August (day 221) 1995.

In the figure at right, results from PRISM using no input data (top panel) and the high elevation data (bottom panel) are compared. The figure shows the ratio of PRISM's calculated slant TEC to the observed TEC along all of the satellite lines-of-sight for that day. The reduction in scatter between the two cases is quite dramatic.

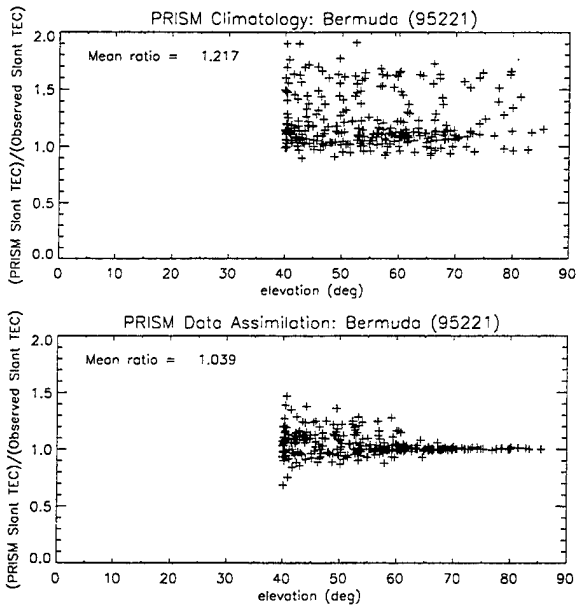

Of course, many more cases using data from a variety of stations and a variety of conditions will be required to draw firm conclusions regarding the efficacy of the PRISM TEC data assimilation algorithm. Since the purpose of these runs was to validate PRISM TEC predictions when driven by TEC input data, no other data (e.g., DISS, SSIES) were used. These calculations also do not test the new TEC data assimilation algorithm described in the previous section. They are simply one part of a comprehensive validation effort that is using data from a variety of sources to thoroughly test PRISM's response to a variety of conditions. That effort will be described by Dr. Decker elsewhere.

4. REFERENCES

Daniell, R. E., and L. D. Brown, PRISM: A Parameterized Real-time Ionospheric Specification Model, Version 1.5, PL-TR-95-2061, May 1995. ADA 299664

Daniell, R. E., W. G. Whartenby, and L. D. Brown, PRISM Validation, PL-TR-94-2198, June 1994. ADA 288476

Daniell, R. E., L. D. Brown, D. N. Anderson, M. W. Fox, P. H. Doherty, D. T. Decker, J. J. Sojka, and R. W. Schunk, Parameterized ionospheric model: A global ionospheric parameterization based on first principles models, *Radio Sci.*, *30*, 1499-1510, 1995.

Daniell, R. E., L. D. Brown, and R. P. Barnes, Modifications and Improvements to the PRISM and PIM Ionospheric Models, AFRL-VS-HA-TR-98-0079, June 1998. ADA 359289

Daniell, R. E., and L. D. Brown, Continued Improvements to the PRISM and PIM Ionospheric Models, AFRL-VS-HA-TR-98-0080, June 1998. ADA 368221

Appendix A
PRISM Updates

Contents: PRISM changes memoranda for the period 20 August 1996 through 10 July 1999.

M·E·M·O·R·A·N·D·U·M

DATE: *13-January-1998*

TO: *Rob Daniell*

FROM: *Lincoln Brown*

RE: *Changes to PRISM 1.7b for PRISM 1.7c*

The changes to PRISM 1.7b for PRISM 1.7c focus improving the midlatitude real-time adjustment algorithm and on replacing the LLF and MLF parameterized models. The changes are summarized as follows:

1. **BUG FIX**: The calculation of the topside half-width of the O^+ density has been corrected. Previously, due to a sign convention error, the topside half-width was calculated as a negative value. It is now correctly calculated as a positive value. Because the minimum of the bottomside and topside half-widths is used by PRISM, and the bottomside O^+ density probably always falls off more rapidly than the topside O^+ density, this bug has probably never influenced the results of PRISM.
2. **BUG FIX**: A minor bug in the selection of magnetic latitudes for interpolation in the MLF parameterized model has been fixed. This bug should not have affected past results.
3. The algorithm for scaling the molecular ion and O^+ model density profiles using simultaneous E-layer and F-layer real-time data corrections has been redesigned. Previously, in the presence of disparate E-layer and F-layer corrections, discontinuities could be introduced into the density profiles, resulting in unintentional changes in peak heights as well as scaled peak densities inconsistent with the real-time data corrections. The new scaling algorithm preserves the heights of the peaks and smoothly transitions the density profile scaling from a pure E-layer correction at the molecular ion density peak height to a pure F-layer correction at the O^+ density peak height.
4. The conversion of TEC real-time data to critical frequency corrections is now based simply on the ratio of data TEC to model TEC, and both f_oF_2 and f_oE corrections are now provided from the conversion. Previously, a more complicated algorithm based on the topside model TEC was used, and only f_oF_2 corrections were provided.
5. Phantom data now no longer influences the sunspot number iteration. Previously, due to the placement of the call to routine PHANTM in the main program, phantom data was generated and included in the real-time data set prior to the sunspot number iteration. Since the sunspot number iteration fits an optimum sunspot number to the real-time data, the phantom data erroneously influenced the outcome of the sunspot number iteration. The call to routine PHANTM has been moved so that the phantom data influences only the midlatitude real-time adjustment.
6. In order to eliminate problems in merging the LLF and MLF parameterized models due to differences between the two theoretical models (LOWLAT and MIDLAT) previously used as

their basis, the LLF and MLF parameterized models have been regenerated from a single theoretical model (LOWLAT). In addition, the following improvements have been made to LOWLAT:

a. The equatorial vertical E×B drift and its radial derivative now vary smoothly to zero in the drift transition region. Previously, a simple linear fall-off was used, resulting in discontinuities in the radial derivative at the drift transition region endpoints.
b. The radial derivative of the equatorial vertical E×B drift is now zero above the drift transition region. Previously, it was never set to zero above the transition region.
c. The dayside and nightside electron temperatures now merge at 0600 and 1800 solar local time. Previously, the electron temperature was discontinuous at 0600 and 1800 solar local time.
d. The neutral wind is now calculated for the correct geographic longitude at all points along a field line. Previously, a fixed geographic longitude was used, resulting in an error in the neutral wind due to the magnetic declination of the field line.

7. The LLF parameterized model has been extended to 44° in absolute latitude, in order to broaden the merge region between the LLF and MLF parameterized models. Previously, the LLF parameterized model only went up to 34° in absolute latitude.
8. The lower absolute latitude boundary of the MLF parameterized model is now 34°, in order to reduce the error due to the assumption of verticality of the midlatitude field lines and to make sure that the midlatitude field lines are outside the region of vertical E×B drift. Previously, the lower absolute latitude boundary of the MLF parameterized model was 30°.
9. The merge region for the LLF and MLF parameterized models has been broadened to the absolute latitude range 34°-44°, in order to improve the quality of the merge. Previously, the range was 30°-34°, too narrow to effectively merge the two parameterized models.
10. Some header comments have been corrected.

The plots at right of f_oF_2 and TEC vs. magnetic latitude illustrate the improvement in PRISM 1.7c regarding the agreement and merging of the LLF and MLF parameterized models. Notice the discontinuities in f_oF_2 and TEC at the LLF/MLF merge region of PRISM 1.7b (±30°-34° magnetic latitude), and their absence in PRISM 1.7c. The plots were generated by PRISM for the following conditions: year 1981, day of the year 173, Universal Time 0000, $F_{10.7}$ 210, K_p 3.5, IMF B_y positive, IMF B_z negative, 270°E magnetic longitude, no URSI f_oF_2

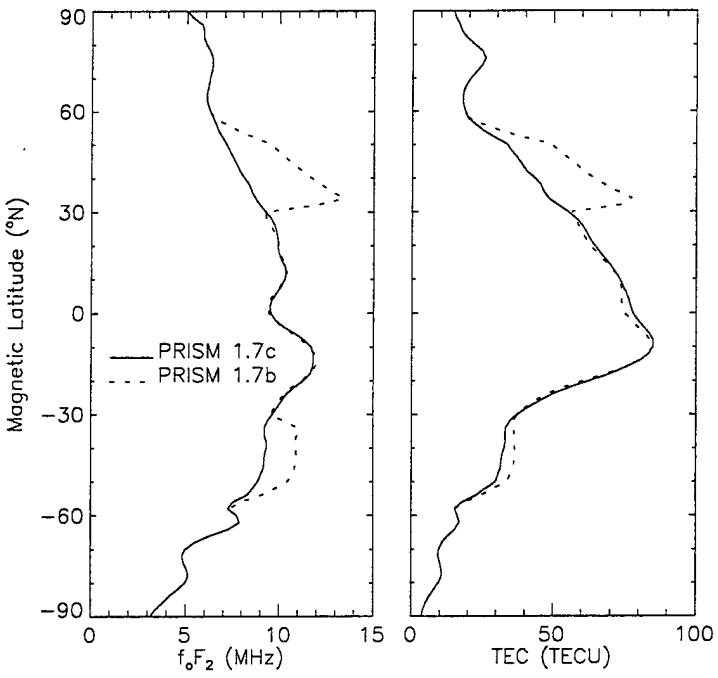

normalization, and no real-time data.

The table below describes the changes that I made to PRISM 1.7b to produce PRISM 1.7c.

Module	Program Unit	Description of Changes
GEN.FOR	Subroutine GENEC	Changed PARAMETER MAXMX from 40 to 50 to accommodate new LLF parameterization.
HLIM.FOR	Subroutine REGMOD	Removed calculations of topside ion column density and critical height difference for TEC data type since they are no longer needed. Removed output parameters TC1 and TC2 since they are no longer used. Removed calculation of n_mF_2 since it is no longer needed. Removed local variable NMF2 since it is no longer needed.
HLISM.FOR	Subroutine MATRIX	Removed arguments TC1 and TC2 from calls to routine REGMOD since they are no longer used by that routine. Removed local variables TC1 and TC2 since they are no longer used.
LOWER.INC	n/a	Changed PARAMETER MOPM1 from 11 to 14 for new LLF parameterization. Changed PARAMETER MX from 35 to 45 for new LLF parameterization.
MID_PARA.FOR	Subroutine MID_F	Corrected test for magnetic latitude above the magnetic latitude grid by changing "(AMLAT .GT. ASMLAT+FLOAT(NMLAT(I,1))*ADMLAT)" to "(AMLAT .GT. ASMLAT+FLOAT(NMLAT(I,1)-1)*ADMLAT)".
MIDLAT.FOR	Subroutine MIDLAT	The conversion of TEC data to critical frequency corrections is now based solely on the ratio of the data TEC to the model TEC, and both f_oF_2 and f_oE corrections are now provided from the conversion process. Removed arguments TC1 and TC2 from calls to routine REGMOD since they are no longer used by that routine. Removed local variables TC1, TC2, W, WFACT, WB, DTEC, TFACT, and NMF2N since they are no longer used. Removed INCLUDE statement for INCLUDE file tomid.inc since it is no longer needed.
MIDLAT.INC	n/a	Changed PARAMETER MX from 12 to 11 for new MLF parameterization.
NEWFIT.INC	n/a	Changed value of PARAMETER MFED from MDISS to MDISS+MIMS to accommodate additional midlatitude f_oE corrections from converted TEC data.
OUTPUT.FOR	Subroutine GRID_OUTPUT	Removed arguments TC1 and TC2 from call to routine REGMOD since they are no longer used by that routine. Removed local variables TC1 and TC2 since they are no longer used.
	Subroutine STATION_OUTPUT	Removed arguments TC1 and TC2 from call to routine REGMOD since they are no longer used by that routine. Removed local variables TC1 and TC2 since they are no longer used.
PARAM.FOR	Subroutine PARAM	Changed lower absolute latitude boundary of pure mid-latitude region from 34. degrees to 44. degrees. Changed upper absolute latitude boundary of low/mid-latitude transition region from 34. degrees to 44. degrees. Changed lower absolute latitude boundary of low/mid-latitude transition region from 30. degrees to 34. degrees. Changed upper absolute latitude boundary of pure low-latitude region from 30. degrees to 34. degrees. Removed comments regarding f_oE normalization from METHOD comment section since no f_oE normalization is done.
PHANTOM.FOR	Subroutine PHANTM	Removed arguments TC1 and TC2 from calls to routine REGMOD since they are no longer used by that routine. Removed local variables TC1 and TC2 since they are no longer used.
PRISM.FOR	Program PRISM	Moved the call to routine PHANTM from after the conversion of the nominal UT from hours to seconds to before the call to routine MIDLAT so that phantom data does not influence the sunspot number iteration. Removed the call to routine INIT that accompanied the call to routine PHANTM since it is no longer needed. Updated the version number and version date.
READ_DBA.FOR	Subroutine LRDOPCF	Changed PARAMETER MOPM1 from 11 to 14 for new LLF parameterization.
RTA.FOR	Subroutine RTA	Removed INCLUDE statement for INCLUDE file tomid.inc since it is not needed.
	Subroutine COR_MAX	Removed arguments EE, EF, FE, FF from the call to routine DO_ADJ since they are no longer needed by that routine.
	Subroutine DO_ADJ	Modified adjustment algorithm to use a unified multiplicative scaling that varies smoothly across altitude boundaries. Removed input parameters NMHME, NMHMF2, NOHME, and NOHMF2 since they are no longer used.
	Subroutine GETHW	Corrected calculation of topside half-width by changing difference HMH-ALTF(J) to ALTF(J)-HMH.

Appendix B. Issues Related to Plasmasphere Modeling

As described in earlier quarterly reports, the question of light ions in GTIM has continued to be of interest. The basic problem is that at very high altitudes, the collision frequency becomes very small. The standard approach to modeling the ionosphere involves the neglect of inertial terms in the momentum equation, so that the equation reduces to a balance between three forces: pressure gradient, gravitation, and friction between the ions and the neutral atmosphere:

$$n_i m_i \upsilon_i \nu_{in} = -\mathbf{b} \cdot \nabla\left(n_i k T_p\right) + n_i m_i \mathbf{g} \cdot \mathbf{b}$$

where **b** is a unit vector in the direction of the magnetic field, $T_p = T_i + T_e$ is the plasma temperature, and I have neglected minor ions (so that $n_i = n_e$). This is valid in the plasmasphere where the dominant ion is H^+. The normal procedure is to divide both sides of the equation by $m_i \nu_{in}$ to obtain an expression for the ion flux, which can be substituted into the continuity equation to obtain the standard diffusion equation. This procedure becomes invalid as $\nu_{in} \to 0$ for the force balance reduces to a balance between the pressure gradient and gravity.

The presence of minor ions (He^+ and O^+) complicates the equation but does not alter the point. We have verified that the matrix resulting from the application of the Crank-Nicholson finite difference scheme is, in fact, ill conditioned, and when solutions are obtained, the ion velocities are often supersonic – a sure sign that the neglect of inertial terms is invalid. Some modelers (e.g., Graham Bailey, personal communication) introduce artificial collisions to keep the equations stable. This may be acceptable as long as the primary interest is below about 3000 km. However, if the quiescent plasmasphere is to be modeled properly, the H^+ densities so obtained are highly questionable.

The Field Line Interhemispheric Plasma (FLIP) model [*Richards and Torr*, 1996] uses the so-called "flux preserving" method [*Torr et al.*, 1990] to model the high altitude (essentially collisionless) plasma and couple it to the low altitude (collisional) plasma of the ionosphere. CPI investigated the possibility of implementing this approach in GTIM, but the numerical scheme for solving the coupled continuity equations for the multiple ion species is fundamentally different from that used in GTIM, so it would be tantamount to developing a completely new code. CPI also investigated the possibility of adapting the fundamental idea – that the condition of continuity of flux implies that the solution of the *steady-state* collisionless momentum equation is mathematically identical to the diffusive equilibrium solution of the collisional continuity equation – to GTIM, but did not have the time nor resources to complete the task.

More recently, *Huba et al.* [1999] and *Joyce and Huba* [1999] have demonstrated the feasibility of solving the coupled continuity and momentum equations *without* neglecting inertial terms. Although numerical solution of these equations requires very short time steps, it appears to yield a stable solution with physically realistic ion velocities even at high altitudes. This approach should be investigated more thoroughly, and consideration given to adopting this for GTIM if modeling of plasmaspheric densities is a desired product.

References:

Huba, J. D., G. Joyce, and J. A. Fedder, SAMI II: A Low Latitude Model of the Ionosphere, Proceedings of IES 99, Alexandria, Virginia, 4-6 May 1999 (in press).

Joyce, G., and J. D. Huba, Development and Results of a New Low-Latitude Ionosphere Model: SAMI 2, presented at the National Radio Science Meeting (URSI), Boulder, Colorado, 4-8 January 1999 (abstract).

Richards, P. G., and D. G. Torr, The Field Line Interhemispheric Plasma Model, in Handbook of Ionospheric Models, R. W. Schunk, ed., SCOSTEP Secretariat, Boulder, Colorado, 1996.

Torr, M. R., D. G. Torr, T. Chang, P. G. Richards, W. Swift, N. Li, *J. Geophys. Res.*, **95**, 21,147, 1990.

Appendix C. PRISM 1.7b and 1.7c Validation Reports

PRISM 1.7b Validation, dated 28 August 1997 begins on the following page.

PRISM 1.7c Validation, dated 13 January 1998 begins on page 24.

PRISM 1.7b Validation

August 28, 1997

Lincoln D. Brown and Robert E. Daniell, Jr.
Computational Physics, Inc.

1. Introduction

This report summarizes the validation of the Parameterized Real-time Ionospheric Specification Model (PRISM) 1.7b. The validation methodology and data set are identical to that used in the validation of PRISM 1.2, as described in PL Technical Report PL-TR-94-2198. Because most of the data used in the validation derives from analog and digital ionosondes, this report concentrates on the validation of the F_2-layer parameters f_oF_2, N_mF_2, and h_mF_2.
Table 1 corresponds to the table in the Executive Summary of the PRISM 1.2 Validation Report. It summarizes the PRISM 1.7b validation and compares it to the performance of PRISM 1.2. In overall performance, PRISM 1.2 and PRISM 1.7b are comparable.

2. f_oF_2 and N_mF_2 Validation

Table 2 summarizes the f_oF_2 and N_mF_2 validation. It corresponds to Table 11 in the PRISM 1.2 Validation Report. PRISM 1.7b shows modest gains over PRISM 1.2 except for the midlatitude driver stations.

3. h_mF_2 Validation

Table 3 summarizes the h_mF_2 validation. It corresponds to Table 16 in the PRISM 1.2 Validation Report. PRISM 1.7b shows substantial improvement over PRISM 1.2 except for the midlatitude driver stations.

4. Discussion

Because PRISM 1.7b has been shown to be comparable in performance to PRISM 1.2, we believe that it is ready for operational status.

Table 1. Summary of PRISM and ICED validation results.

Quantity	RMS Error			Improvement over ICED (%)	
	ICED	PRISM 1.2	PRISM 1.7b	PRISM 1.2	PRISM 1.7b
f_oF_2 (MHz)	1.5	0.7	0.6	54	58
N_mF_2 (%)	40	20	19	50	54
h_mF_2 (km)	25	6	8	75	69

Table 2. Summary of f_oF_2 and N_mF_2 validation results.

Quantity	RMS Error			Improvement over ICED (%)	
	ICED	PRISM 1.2	PRISM 1.7b	PRISM 1.2	PRISM 1.7b
Midlatitude Statistics					
All Stations					
f_oF_2 (MHz)	1.5	0.5	0.6	63	61
N_mF_2 (%)	36	17	16	53	55
Driver Stations					
f_oF_2 (MHz)	1.6	0.0	0.2	97	86
N_mF_2 (%)	39	1	6	97	86
Ground-Truth Stations					
f_oF_2 (MHz)	1.1	1.0	1.0	10	11
N_mF_2 (%)	29	30	28	-6	5
Global Statistics					
All Stations					
f_oF_2 (MHz)	1.5	0.7	0.6	54	58
N_mF_2 (%)	40	20	19	50	54
Driver Stations					
f_oF_2 (MHz)	1.6	0.4	0.4	73	77
N_mF_2 (%)	44	13	12	70	74
Ground-Truth Stations					
f_oF_2 (MHz)	1.1	1.0	1.0	5	11
N_mF_2 (%)	30	31	29	-5	4

Table 3. Summary of h_mF_2 validation results for 9 October.

	RMS Error (km)			Improvement over ICED (%)	
	ICED	PRISM 1.2	PRISM 1.7b	PRISM 1.2	PRISM 1.7b
Global Statistics					
Driver Stations	27	24	9	11	67
Other (Ground-Truth)	20	13	11	35	44
All	25	22	9	12	64
Midlatitude Statistics					
Driver Stations	27	0	6	99	75
Other (Ground-Truth)	20	13	11	36	44
All	25	6	8	75	69

PRISM 1.7c Validation

January 13, 1998

Lincoln D. Brown and Robert E. Daniell, Jr.
Computational Physics, Inc.

1. Introduction

This report summarizes the validation of the Parameterized Real-time Ionospheric Specification Model (PRISM) 1.7c. The validation methodology and data set are identical to that used in the validation of PRISM 1.2 and PRISM 1.7b. The validation of PRISM 1.2 is described in PL Technical Report PL-TR-94-2198 entitled *PRISM Validation*. The validation of PRISM 1.7b is described in the CPI report entitled *PRISM 1.7b Validation*. Because most of the data used in the validation derives from analog and digital ionosondes, this report concentrates on the validation of the F_2-layer parameters f_oF_2, N_mF_2, and h_mF_2, but it also includes validation of *TEC*.
Table 1 corresponds to the table in the Executive Summary of the PRISM 1.2 validation report, and to Table 1 in the PRISM 1.7b validation report. It summarizes the PRISM 1.7c validation and compares it to the performance of PRISM 1.2 and PRISM 1.7b. In overall performance, PRISM 1.7c is comparable to PRISM 1.2 and substantially improved over PRISM 1.7b in *TEC* prediction.

2. f_oF_2 and N_mF_2 Validation

Table 2 summarizes the f_oF_2 and N_mF_2 validation. It corresponds to Table 11 in the PRISM 1.2 validation report, and to Table 2 in the PRISM 1.7b validation report. PRISM 1.7c shows modest gains over PRISM 1.2 except for the midlatitude ground-truth stations, where the difference is statistically small. PRISM 1.7c correctly reproduces midlatitude driver f_oF_2 and N_mF_2, an improvement over PRISM 1.7b.

3. h_mF_2 Validation

Table 3 summarizes the h_mF_2 validation. It corresponds to Table 16 in the PRISM 1.2 validation report, and to Table 3 in the PRISM 1.7b validation report. PRISM 1.7c shows substantial improvement over PRISM 1.2, especially in the global sense. PRISM 1.7c correctly reproduces midlatitude driver h_mF_2, an improvement over PRISM 1.7b.

4. *TEC* Validation

Table 4 summarizes the *TEC* validation. It corresponds to Table 17 in the PRISM 1.2 validation report. PRISM 1.7c shows substantial improvement over PRISM 1.2 and 1.7b in predicting *TEC* away from driver data. PRISM 1.7c closely reproduces driver *TEC*, which gives us confidence in its electron density height distribution.

5. Discussion

Because PRISM 1.7c has been shown to be comparable in performance to PRISM 1.2, and in detail improved over PRISM 1.2 in *TEC* performance, we believe that it is ready for operational status.

Table 1. Summary of PRISM and ICED validation results.

Quantity	RMS Error				Improvement over ICED (%)		
	ICED	PRISM 1.2	PRISM 1.7b	PRISM 1.7c	PRISM 1.2	PRISM 1.7b	PRISM 1.7c
f_oF_2 (MHz)	1.5	0.7	0.6	0.6	54	58	58
N_mF_2 (%)	40	20	19	18	50	54	56
h_mF_2 (km)	25	6	8	5	75	69	78
TEC (TECU)	7.3	3.0	4.9	1.6	75	32	78

Table 2. Summary of f_oF_2 and N_mF_2 validation results.

Quantity	RMS Error				Improvement over ICED (%)		
	ICED	PRISM 1.2	PRISM 1.7b	PRISM 1.7c	PRISM 1.2	PRISM 1.7b	PRISM 1.7c
Midlatitude Statistics							
All Stations							
f_oF_2 (MHz)	1.5	0.5	0.6	0.6	63	61	61
N_mF_2 (%)	36	17	16	16	53	55	57
Driver Stations							
f_oF_2 (MHz)	1.6	0.0	0.2	0.0	97	86	100
N_mF_2 (%)	39	1	6	0	97	86	100
Ground-Truth Stations							
f_oF_2 (MHz)	1.1	1.0	1.0	1.0	10	11	5
N_mF_2 (%)	29	30	28	28	-6	5	5
Global Statistics							
All Stations							
f_oF_2 (MHz)	1.5	0.7	0.6	0.6	54	58	58
N_mF_2 (%)	40	20	19	18	50	54	56
Driver Stations							
f_oF_2 (MHz)	1.6	0.4	0.4	0.3	73	77	81
N_mF_2 (%)	44	13	12	10	70	74	77
Ground-Truth Stations							
f_oF_2 (MHz)	1.1	1.0	1.0	1.0	5	11	5
N_mF_2 (%)	30	31	29	29	-5	4	4

Table 3. Summary of h_mF_2 validation results for 9-October.

	RMS Error (km)				Improvement over ICED (%)		
	ICED	PRISM 1.2	PRISM 1.7b	PRISM 1.7c	PRISM 1.2	PRISM 1.7b	PRISM 1.7c
Global Statistics							
Driver Stations	27	24	9	5	11	67	83
Other (Ground-Truth)	20	13	11	11	35	44	44
All	25	22	9	7	12	64	74

Midlatitude Statistics							
Driver Stations	27	0	6	0	99	75	100
Other (Ground-Truth)	20	13	11	11	36	44	44
All	25	6	8	5	75	69	78

Table 4. Summary of *TEC* validation results.

	RMS Error (TECU)				Improvement over ICED (%)		
	ICED	PRISM 1.2	PRISM 1.7b	PRISM 1.7c	PRISM 1.2	PRISM 1.7b	PRISM 1.7c
Driver Stations	8.1	0.3	0.1	0.1	94	98	99
Other (Ground-Truth)	3.7	6.3	9.7	3.2	-25	-158	16
All	7.3	3.0	4.9	1.6	75	32	78